Dose-Dependent Inhibition of Tobacco Smoke Carcinogen–Induced Lung Tumorigenesis in A/J Mice by Indole-3-Carbinol

Fekadu Kassie, Ilze Matise, Mesfin Negia, Pramod Upadhyaya and Stephen S. Hecht

Abstract Recently, we reported inhibition of 4-(methylnitrosamino)-1-(3-pyridyl)-1-butanone (NNK) plus benzo(*a*)pyrene (BaP)–induced lung tumorigenesis in A/J mice by indole-3-carbinol (I3C; 112 μmol/g diet) administered beginning at 50% in the carcinogen treatment phase. In this study, we examined the dose-dependent and postcarcinogen tumor-inhibitory activities of I3C. A mixture of NNK plus BaP (2 μmol each) administered by gavage as eight biweekly doses caused 21.1 ± 5.2 lung tumors per mouse. Carcinogen-treated mice given diets containing I3C at 1, 10, 30, 71, and 112 μmol/g, beginning at 50% in the carcinogen treatment phase, had 17.9 ± 6.1, 10.4 ± 3.7, 9.8 ± 5.1, 5.2 ± 4.0, and 2.5 ± 2.4 lung tumors per mouse, corresponding to reductions by 15%, 51%, 53%, 75%, and 88%, respectively. All reductions, except at the lowest dose level (1 μmol I3C/g diet), were significant ($P < 0.001$). Similarly, administration of I3C (112 μmol/g diet) beginning 1 week after the last dose of the carcinogen significantly reduced NNK plus BaP-induced lung tumor multiplicity to 5.6 ± 3.5, corresponding to a reduction by 74%. Analyses of cell proliferation and apoptosis markers revealed that I3C reduced the number of Ki-67–positive cells and expression of proliferating cell nuclear antigen, phospho-Akt, and phospho-BAD and increased cleavage of poly(ADP-ribose) polymerase, suggesting that the lung tumor inhibitory effects of I3C were mediated, at least partly, through inhibition of cell proliferation and induction of apoptosis. These results clearly show the efficacy of I3C in the prevention of tobacco carcinogen–induced lung tumorigenesis in A/J mice and provide a basis for future evaluation of this compound in clinical trials as a chemopreventive agent for current and former smokers.

Lung cancer is the most common cause of death from cancer worldwide (1). In the United States, an estimated 215,020 new cases and 161,840 deaths were expected in 2008, accounting for 15% of cancer diagnoses and 29% of all cancer deaths, respectively (2). Cigarette smoke, which contains >60 carcinogens, is the cause of ~90% of lung cancer cases (3, 4). The tobacco-specific nitrosamine 4-(methylnitrosamino)-1-(3-pyridyl)-1-butanone (NNK) and benzo(*a*)pyrene (BaP), a prototypical polycyclic aromatic hydrocarbon, are two of the most potent tobacco smoke carcinogens in rodent models and are strongly implicated in the etiology of lung cancer in smokers (4, 5). NNK and BaP, individually or in combination, have been used frequently to induce lung tumors in A/J mice, inducing 10 to 30 or more tumors per lung with a 100% tumor incidence (6). The morphology, histology, and molecular characteristics of mouse lung tumors are similar to human lung adenocarcinoma, the most common type of human lung cancer (7, 8). Therefore, this mouse model of lung tumorigenesis is well suited for the identification of chemopreventive agents that could prevent lung cancer in current and former smokers.

Indole-3-carbinol (I3C) occurs in commonly consumed cruciferous vegetables as indole glucosinolate (glucobrasscin). About four different glucobrassicins have been identified in cruciferous vegetables and, of these, indolylmethyl (glucobrassicin) and 1-methoxy-3-indolylmethyl (neoglucobrassicin) are found frequently (9). Upon hydrolysis by the plant enzyme myrosinase, when plant cells are damaged, glucobrassicins yield predominantly I3C or related substituted I3Cs (10). If plant myrosinase is inactivated (e.g., with cooking), glucobrassicins can be degraded in the gastrointestinal tract by the intestinal microflora, albeit at a lower level (11). In the stomach, I3C undergoes condensation reactions to produce various products, the major one being 3,3-diindolylmethane (12). Most of the biological activities of I3C are attributed to 3,3-diindolylmethane (13). The dietary intake of glucobrassicins is much higher than that of alkyl and aralkyl glucosinolates, the other group of glucosinolates that yield isothiocyanates upon hydrolysis. We previously reported that glucobrassicins were the predominant glucosinolates in seven of nine vegetables consumed by Singapore Chinese, accounting for 70.0% to 93.2% of all glucosinolates detected (14). In the United States

Authors' Affiliation: Masonic Cancer Center, University of Minnesota, Minneapolis, Minnesota

Received 04/04/2008; revised 06/06/2008; accepted 07/02/2008.

Grant support: NIH/National Cancer Institute grant CA-102502 (S.S. Hecht).

Requests for reprints: Fekadu Kassie, Masonic Cancer Center, University of Minnesota, Mayo Mail Code 806, 420 Delaware Street Southeast, Minneapolis, MN 55455. Phone: 612-626-5143; Fax: 612-626-5135; E-mail: kassi012@umn.edu.

doi:10.1158/1940-6207.CAPR-08-0064

and the United Kingdom, estimated per capita intakes of glucobrassicin are 8.1 and 19.4 mg/d, respectively (15, 16), whereas in some populations in Asia, the level reaches 46 mg/d (14).

Considerable evidence shows that I3C inhibits experimentally induced tumorigenesis in murine models at different sites, including lung, through induction of phase I and phase II enzymes, inhibition of proliferation and induction of apoptosis in tumor cells, and modulation of estrogen metabolism (9). In humans, preliminary studies indicate that I3C is effective for the treatment of cervical intraepithelial hyperplasia (17) and recurrent respiratory papillomatosis (18). In a phase I clinical trial, daily administration of I3C at doses of 400 and 800 mg increased levels of glutathione-*S*-transferase and P450 1A2 and increased the ratio of 2-:16α-hydroxyestrone without causing any toxic effects (19). At times, dietary supplements of I3C in the form of capsules have been sold regularly by drug stores and health food stores. Despite its potent antitumor activity, I3C promotes chemically induced hepatic tumorigenesis depending on the initiator, exposure protocol, and species of test animal (20).

Recently, we reported inhibition of NNK plus BaP–induced lung tumorigenesis in A/J mice by I3C administered beginning at 50% in the carcinogen treatment phase (21). In the present study, we sought to examine the dose-dependent tumor-inhibitory effects of I3C and to determine if administration of the compound during the postcarcinogen treatment phase also inhibits lung tumorigenesis.

Materials and Methods

Chemicals, reagents, and diets

The protease inhibitor cocktail, BaP, and I3C were from Sigma. NNK was synthesized (22). Mouse diets (AIN-93G and AIN-93M) were purchased from Harlan Teklad. The AIN-93G diet, high in protein and fat, was used to support rapid growth of the mice during early age, whereas AIN-93M diet, low in protein and fat, was used for adult maintenance (23).

Stability of I3C in the diet

Before assessing the chemopreventive activity of I3C, we determined its stability under conditions in which the I3C-supplemented diets were stored or given to the mice. One-gram samples of I3C-supplemented diet were taken from a diet that had been stored at 4°C for 4 wk or kept in the metal feeders in the mouse cages for 4 d. The diet was extracted with acetonitrile by sonication for 5 min and centrifuged at 2,800 rpm for 3 min; the supernatant was then removed and the solvent was evaporated under a gentle stream of N_2. The residue was redissolved in acetonitrile and analyzed by high-performance liquid chromatography with a Waters Associates system equipped with a model 440 UV detector. Samples were loaded onto a 300 mm × 3.9 mm, 10 μm C18 Bondclone (Phenomenex) column and eluted at 0.5 mL/min with 5% acetonitrile in H_2O to 100% acetonitrile for 40 min. Detection was by UV (254 nm). The retention time of I3C was 29.4 min.

Animal studies

Two animal studies were carried out. In experiment 1, the efficacy of I3C for chemoprevention of lung tumorigenesis was determined. Experiment 2 was done to harvest tissues for Western assays.

Experiment 1. Female A/J mice, 5 to 6 weeks of age, were obtained from The Jackson Laboratory. Although both female and male A/J mice develop lung tumors equally (24), female mice are easier to handle. The experimental design is shown in Fig. 1. Upon arrival, the mice were housed in the specific pathogen-free animal quarters of Research Animal Resources, at the University of Minnesota Academic Health Center. The mice were randomized into different groups (group 1, carcinogen only treated; groups 2 to 7, carcinogen and I3C treated; group 8, I3C only treated; group 9, vehicle treated) and maintained on AIN-93G pelleted diet. One week after arrival, the mice were switched to AIN-93G powdered diet and treated by gavage with either a mixture of BaP plus NNK (2 μmol of each, groups 1-7) in 0.1 mL cottonseed oil or cottonseed oil alone (groups 8 and 9), twice weekly for eight treatments. Mice in groups 2 to 7 were given I3C in the diet beginning at either 1 d after the fourth treatment with the carcinogens (groups 2-6, temporal sequence A) or 1 wk after the last carcinogen treatment (group 7, temporal sequence B) until termination of the study at week 27 (Table 1). Mice in group 8 were given I3C-supplemented diet for the same duration as mice in groups 2 to 6.

The powdered diet was administered using metal box feeders (Lab Products, Inc.), which allowed monitoring of food consumption and minimized diet waste. Fresh diet was provided every 3 to 4 d. Food consumption was monitored twice a week. Body weight and water consumption were recorded every week. The mice were sacrificed at week 27 of the experiment. Immediately upon sacrifice, lungs were perfused with cold PBS and harvested, and tumors were scored using a dissecting microscope. During the tumor count, the lungs were protected from drying by moistening them with PBS. Lungs from 50% of the mice per group were preserved in 10% buffered formalin. Lung tumors from the remaining mice were microdissected and kept at −80°C. Mice perirenal fats were removed and weighed at the end of the experiment.

Experiment 2. This experiment was carried out to harvest lung tissues for Western immunoblotting studies. Female A/J mice were randomly assigned to three groups, 6 mice each, and maintained on AIN-93G diet: group 1, NNK plus BaP treated; group 2, NNK plus BaP and I3C treated; group 3, vehicle treated. Mice in groups 1 and 2 were gavaged with eight biweekly doses of a mixture of NNK plus BaP (2 μmol of each) in 0.1 mL cottonseed oil; mice in group 3 received the vehicle only. Beginning at 1 wk after the last dose of the

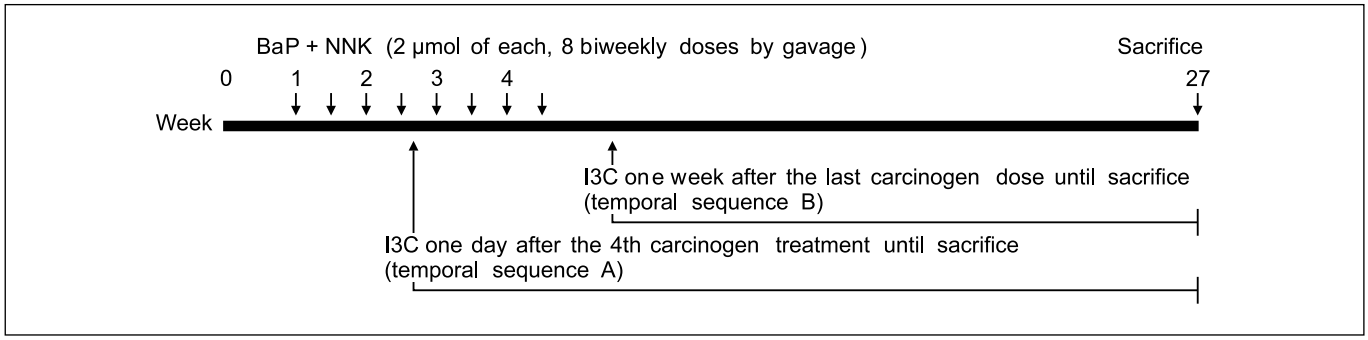

Fig. 1. Experimental design to assess inhibition of NNK plus BaP–induced lung tumorigenesis in A/J mice by I3C.

Table 1. Dose-dependent inhibition of NNK plus BaP-induced lung tumorigenesis by I3C in A/J mice

Group	Temporal sequence	I3C (dose, μmol/g diet)	Carcinogen	No. mice		Mean body weight at termination (g ± SD)	Lung tumors			
				Initial	At termination		Tumor incidence (%)	Tumors/ mouse (mean ± SD)	Reduction in tumor multiplicity (%)	*P**
1	—	—	NNK + BaP	17	17	23.8 ± 2.2	100	21.1 ± 5.2		
2	A	112	NNK + BaP	13	12	19.3 ± 2.2	85	2.5 ± 2.4	88	<0.0001
3	A	71	NNK + BaP	14	14	20.8 ± 1.6	86	5.2 ± 4.0	75	<0.0001
4	A	30	NNK + BaP	15	14	21.2 ± 1.4	100	9.8 ± 5.1	53	<0.0001
5	A	10	NNK + BaP	18	18	22.4 ± 2.8	100	10.4 ± 3.7	51	<0.0001
6	A	1	NNK + BaP	18	17	22.8 ± 2.2	100	17.9 ± 6.1	15	0.19
7	B	112	NNK + BaP	15	15	19.6 ± 2.6	100	5.6 ± 3.5	74	<0.0001
8	—	112†	None	12	10	19.9 ± 2.0	0	0	—	
9	—	None	None	10	10	25.7 ± 2.4	20	0.2 ± 0.4	—	

NOTE: Beginning at age 6 to 7 wk, groups of female A/J mice were gavaged with eight biweekly doses of a mixture of NNK + BaP (2 μmol each) in 0.1 mL cottonseed oil. The mice were maintained on AIN-93G diet from age 5 to 6 wk until 1 wk after the end of carcinogen treatment, then shifted to AIN-93M diet for the duration of the experiment. I3C was added to the diet beginning at 1 d after the fourth treatment with the carcinogens or 1 wk after the last carcinogen treatment. The experiment was terminated 27 wk after the first dose of the carcinogens.

*Compared with group 1.

†The duration of I3C administration was as for mice in groups 2 to 6.

carcinogens, the diet of the mice in group 2 was supplemented with I3C (112 μmol/g diet). At week 13 of the experiment, the mice were sacrificed and the lungs were harvested and snap frozen in liquid nitrogen.

Immunohistochemical analysis

To assess Ki-67 and phospho-Akt expression in lung tissues (groups 1, 7, and 9) obtained from experiment 1, 4 μm formalin-fixed paraffin sections were deparaffinized and antigen retrieved by incubating the slides in a pressure cooker in citrate buffer (pH 6.0) for 30 s at 121°C and 10 s at 90°C followed by cooling for 15 min. Endogenous peroxidase was blocked with 3% hydrogen peroxide for 15 min at room temperature. The sections were incubated with a universal protein block (DAKO) for 10 min, followed by a 60-min, room temperature incubation with rat monoclonal antibody specific to mouse Ki-67 (DAKO) or phospho-Akt (Ser^{473}). Sections were then incubated for 30 min at room temperature with biotinylated anti-rat secondary antibody (Vector) diluted at 1:300. Binding was detected by incubating sections with streptavidin/horseradish peroxidase (DAKO) for 20 min at room temperature followed by diaminobenzidine chromagen application for 5 min at room temperature. Sections were counterstained with Mayer's hematoxylin (DAKO). For negative control slides, the primary antibody was substituted by Super Sensitive Negative Control Rat serum (Biogenix). For Ki-67 analysis, images were captured with an attached camera linked to a computer and the Ki-67 labeling index was calculated as the percentage of Ki-67–positive tumor cells that showed brown nuclear staining among 1,700 tumor cells counted in seven fields. For determination of phospho-Akt labeling index, tumor areas that stained brown were selected, and the percent area of tumor that stained brown was calculated using Image Pro software. A total of 9 and 16 tumors were analyzed for carcinogen + I3C and carcinogen only group, respectively.

Western immunoblot analyses

Aliquots of lung tissues (30 mg tissue per mouse, six mice per group, from vehicle group of experiment 1 or all groups in experiment 2) or pooled lung tumors (a total of 180 mg from 6 mice in the carcinogen alone group or carcinogen plus I3C group, postcarcinogen, in experiment 1) were homogenized in ice-cold lysis buffer [50 mmol/L Tris-HCl, 150 mmol/L NaCl, 1 mmol/L EGTA, 1 mmol/L EDTA, 20 mmol/L, 1% Triton X-100 (pH 7.4)] containing protease inhibitors [aprotinin (1 μg/mL), leupeptin (1 μg/mL), pepstatin (1 μmol/L), and phenylmethylsulfonyl fluoride (0.1 mmol/L)] and the phosphatase inhibitors Na_3VO_4 (1 mmol/L) and NaF (1 mmol/L). After the homogenates had been centrifuged (14,000 × *g* for 25 min at 4 °C) and the supernatants were collected, aliquoted, and stored at −80 °C. For Western immunoblotting, 60 μg of protein per sample were loaded onto a 4% to 12% Novex Tris-glycine gel (Invitrogen) and run for 60 min at 200 V. The proteins were then transferred onto a nitrocellulose membrane (Bio-Rad) for 1 h at 30 V. Protein transfer was confirmed by staining membranes with BLOT-FastStain (Chemicon). Subsequently, membranes were blocked in 5% Blotto nonfat dry milk in Tris buffer containing 1% Tween 20 for 1 h and probed overnight with the following primary antibodies: anti-Akt (1:1,000), anti–phospho-Akt Ser^{473} (1:1,000), anti–phospho-BAD Ser^{155} (1:1,000), anti–proliferating cell nuclear antigen (PCNA, 1:1,000), and anti–poly(ADP-ribose) polymerase (PARP; 1:1,000). After incubating the membranes with a secondary antibody (goat anti-rabbit IgG, 1:20,000, Santa Cruz Biotechnology) for 1 h, chemiluminescent immunodetection was used. The signal was visualized by exposing membranes to HyBolt CL autoradiography film. Membranes were stripped and probed with anti–β-actin to check for differences in the amount of protein loaded in each lane. The experiment was carried out twice using the same tissue lysates.

Statistical analyses

The results of gross tumor counts were summarized as mean and SD for the different groups defined by the doses of I3C. The data were further divided according to the temporal sequence of I3C administration. The effects of I3C are reported as a percent change in tumor multiplicity in carcinogen and chemopreventive agent-treated groups relative to the groups treated with carcinogen only. Statistical comparisons among the groups were done using Poisson regression, which is specific for data representing counts or number of events and can handle cases where few or no events occur. A *P* value of

<0.01 was used to judge statistical significance. Student's *t* test was used to compare protein expression levels and Ki-67 and phosphor-Akt labeling index among the different lung tissues.

Results

I3C was stable under the conditions of storage or feeding

As seen in Fig. 2B, I3C was stable when kept at 4°C for 1 month. When left in the mouse feeders in the open for 4 days, ~5% of the parent compound was degraded to 3,3-diindolylmethane (Fig. 2C).

I3C caused hyperphagia and reductions in body weight gain and perirenal fat pad weights

Observation of the mice once a week for signs of toxicity, such as changes in fur color or texture, motor and behavioral abnormalities, and palpable masses, did not reveal any of these effects. Food consumption and body weight curves of the mice are depicted in Fig. 3. After an initial decline, the average food consumption of mice maintained on I3C-supplemented diet increased in a dose-dependent manner (by 2%, 4%, 7%, 11%, and 13% at doses of 1, 10, 30, 71, and 112 μmol I3C/g diet, respectively, compared with the group treated with carcinogens alone and maintained on nonsupplemented diet) and the effects at 71 and 112 μmol/g diet were significant ($P < 0.05$; Fig. 3A). Despite the increased food consumption, mice maintained on I3C-supplemteted diet had lower body weights compared with mice given the nonsupplemented diet. For example, upon termination of the study at week 27, the body weight of mice given 10, 30, 71, and 112 μmol I3C/g diet decreased by 4%, 6%, 8%, 13%, and 16%, respectively. The effects of 71 and 112 μmol I3C/g diet were significant ($P < 0.05$; Fig. 3A). Consistent with the decrease in body weight, the amount of perirenal adipose tissue in I3C-treated mice was reduced in a dose-dependent manner (decreased by 2%, 6%, 14%, 38%, and 85% at doses of 1, 10, 30, 71, and 112 μmol I3C/g diet, respectively, Fig. 3B).

I3C reduced NNK plus BaP–induced lung tumor multiplicity in a dose-dependent fashion

Mice treated with NNK plus BaP and fed nonsupplemented diet had 21.1 ± 5.2 lung tumors per mouse. Carcinogen-treated mice given diets containing I3C at 1, 10, 30, 71, and 112 μmol/g diet, beginning at 50% in the carcinogen treatment phase, had 17.9 ± 6.1, 10.4 ± 3.7, 9.8 ± 5.1, 5.2 ± 4.0, and 2.5 ± 2.4 tumors per mouse, corresponding to reductions by 15%, 51%, 53%, 75%, and 88%, respectively (Table 1). All reductions, except at the lowest dose level (1 μmol I3C/g diet), were significant ($P < 0.001$). Similarly, administration of I3C at a dose level of 112 μmol/g diet, beginning 1 week after the last dose of the carcinogen, significantly reduced NNK plus BaP–induced lung tumor multiplicity to 5.6 ± 3.5 ($P < 0.001$), corresponding to reduction by 74%. No tumors were observed in the group treated with I3C alone, whereas the lung tumor multiplicity in the vehicle control group was within the range of historical controls (0.20 ± 0.42 tumors per mouse). Tumor incidence was not significantly reduced by I3C. This was not unexpected because the most sensitive indicator in the A/J mouse lung tumorigenesis model is tumor multiplicity.

Inhibition of cell proliferation and induction of apoptosis in lung cells from I3C-treated mice

To assess potential mechanisms involved in the lung tumor inhibitory effects of I3C when given during the postcarcinogen treatment phase, we analyzed the levels in lung tissues of proteins involved in cell proliferation and apoptosis using immunohistochemistry and Western immunoblotting.

Immunohistochemical staining for Ki-67, a marker of cell proliferation, showed that Ki-67 was expressed only in 0.2% of lung cells from vehicle-treated mice. On the other hand, nuclear staining for Ki-67 was seen in numerous neoplastic cells (9.6%) within pulmonary adenoma of carcinogen-treated mice. In mice treated with the carcinogens and given I3C (112 μmol/g diet), the level of Ki-67 was significantly reduced (2.2%) relative to the level in mice treated with the carcinogens alone (Fig. 4A and B), indicating reduction in the rate of cell proliferation in lung tumors of mice maintained on I3C-supplemented diet.

As seen in Fig. 4A, there was a weak expression of phospho-Akt in bronchiolar epithelial cells and pulmonary macrophages of vehicle-treated mice. In mice treated with the carcinogens alone, there was weak to moderate intracytoplasmic staining of neoplastic epithelial cells in most adenoma. However, in a few adenoma, there was a higher intensity of

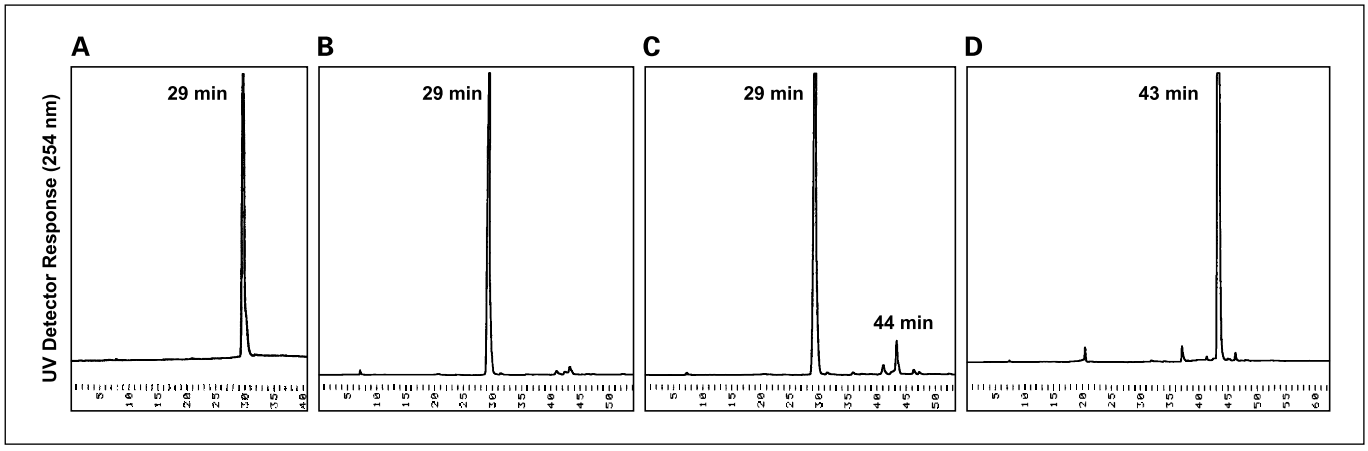

Fig. 2. High-performance liquid chromatography analysis of I3C-supplemented AIN-93 mouse diet. *A*, I3C standard. *B*, I3C-supplemented diet kept at 4°C for 1 mo. *C*, I3C-supplemented diet kept in the mouse feeders in the open for 4 d. *D*, 3,3-diindolylmethane standard.

cytoplasmic staining localized to areas of tumors containing pleomorphic neoplastic cells (Fig. 4A). In mice treated with the carcinogens and given I3C (112 μmol/g diet), staining for phospho-Akt in neoplastic cells of adenoma was weak to moderate with only a rare focus of more intense staining limited to areas of pleomorphic epithelial cells. In all tissue samples, phospho-Akt staining was completely absent when phospho-Akt antibody was incubated with specific phospho-Akt blocking peptide. These results suggest that phospho-Akt is expressed at higher levels in tumors that exhibit increased cellular pleomorphism and that in I3C-treated mice the number of such tumors is reduced. However, quantification of the number of phospho-Akt–positive cells, using Image Pro, did not show significant differences between the carcinogen-only group and that of the group treated with carcinogens and I3C (Fig. 4B).

To further assess the effect of I3C on cell proliferation and survival-related proteins, we determined expression levels of phospho-Akt, PCNA, a marker of cell proliferation, and phospho-BAD, a downstream target of phospho-Akt, and cleavage of PARP using Western immunoblotting. In both experiment 1 (27 weeks study) and experiment 2 (13 weeks study), the levels of these proteins increased in lung tissues of carcinogen-treated versus vehicle-treated mice (Figs. 4C and D). However, upon supplementation of the diet of carcinogen-treated mice with I3C, levels of phospho-Akt, PCNA, and phospho-BAD decreased and cleavage of PARP increased (Figs. 4C and E), suggesting that I3C inhibits cell proliferation and survival in preneoplastic/tumor cells of the lung.

Discussion

Previously, we reported inhibition of NNK plus BaP–induced lung tumorigenesis in A/J mice by I3C (112 μmol/g diet) given beginning at 50% in the carcinogen treatment phase (21). In the present study, we further investigated the lung tumor inhibitory effects of I3C by administering the compound at different dose levels and temporal sequences. The results show that I3C given at doses of 1, 10, 30, 71, and 112 μmol/g diet beginning at 50% in the carcinogen treatment phase or at the dose of 112 μmol/g diet during the postcarcinogen treatment phase caused significant reductions (except at the dose level of 1 μmol I3C/g diet) in NNK plus BaP–induced lung tumor multiplicity. The lung tumor inhibitory effects of I3C observed on administration of the compound during the postcarcinogen treatment phase are likely to be associated with a combination of reduced cell proliferation and induced apoptosis. Our findings are highly relevant for future research on the lung cancer–chemopreventive effects of I3C in smokers and ex-smokers.

The mean body weights of mice maintained on I3C-supplemented diets were reduced by 4% to 19% relative to the group given conventional AIN-93 diet. Moreover, I3C

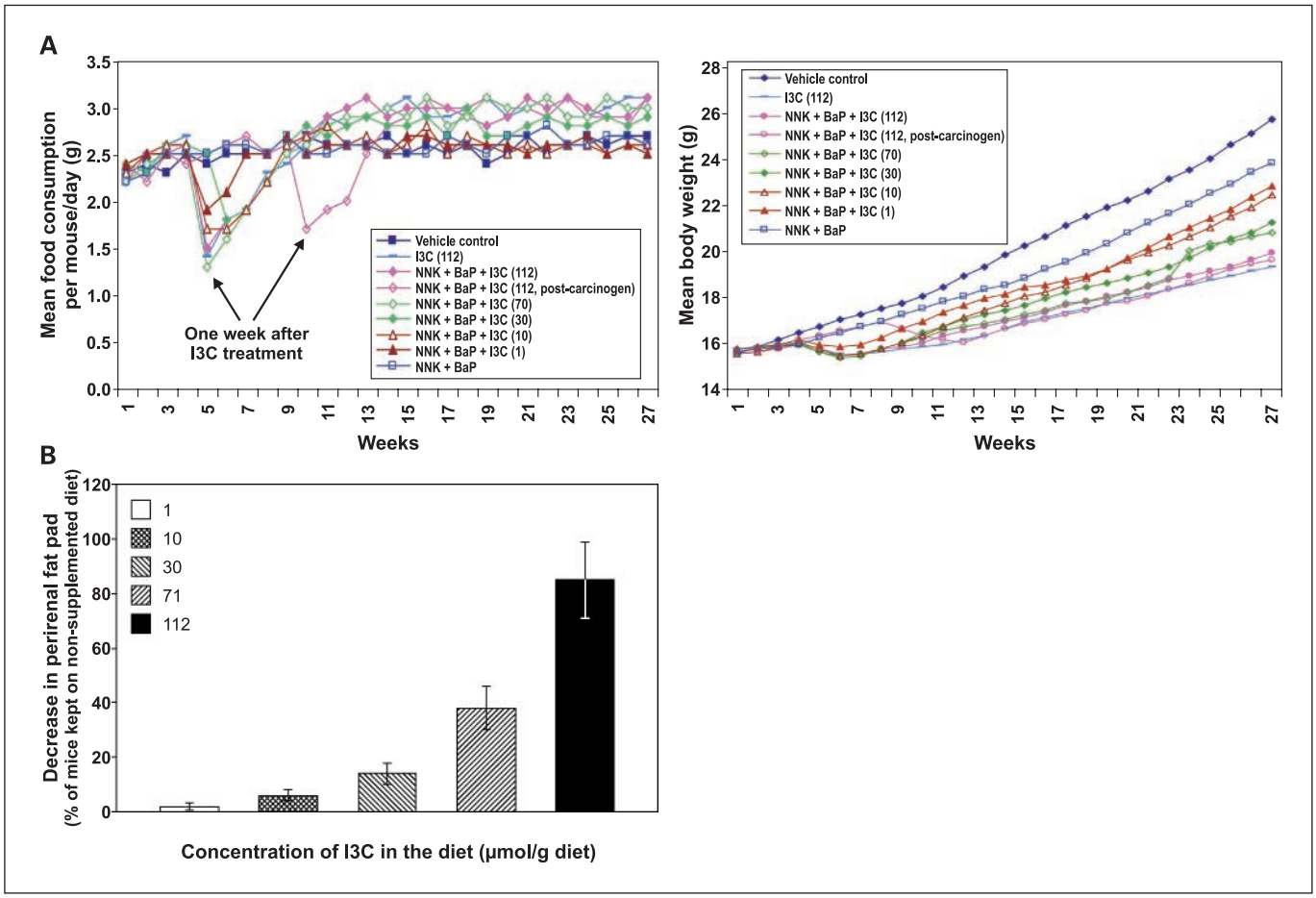

Fig. 3. *A,* effect of I3C on food consumption (*left*) and body weight gain (*right*) of female A/J mice. *B,* dose-dependent reduction of perirenal fat by I3C.

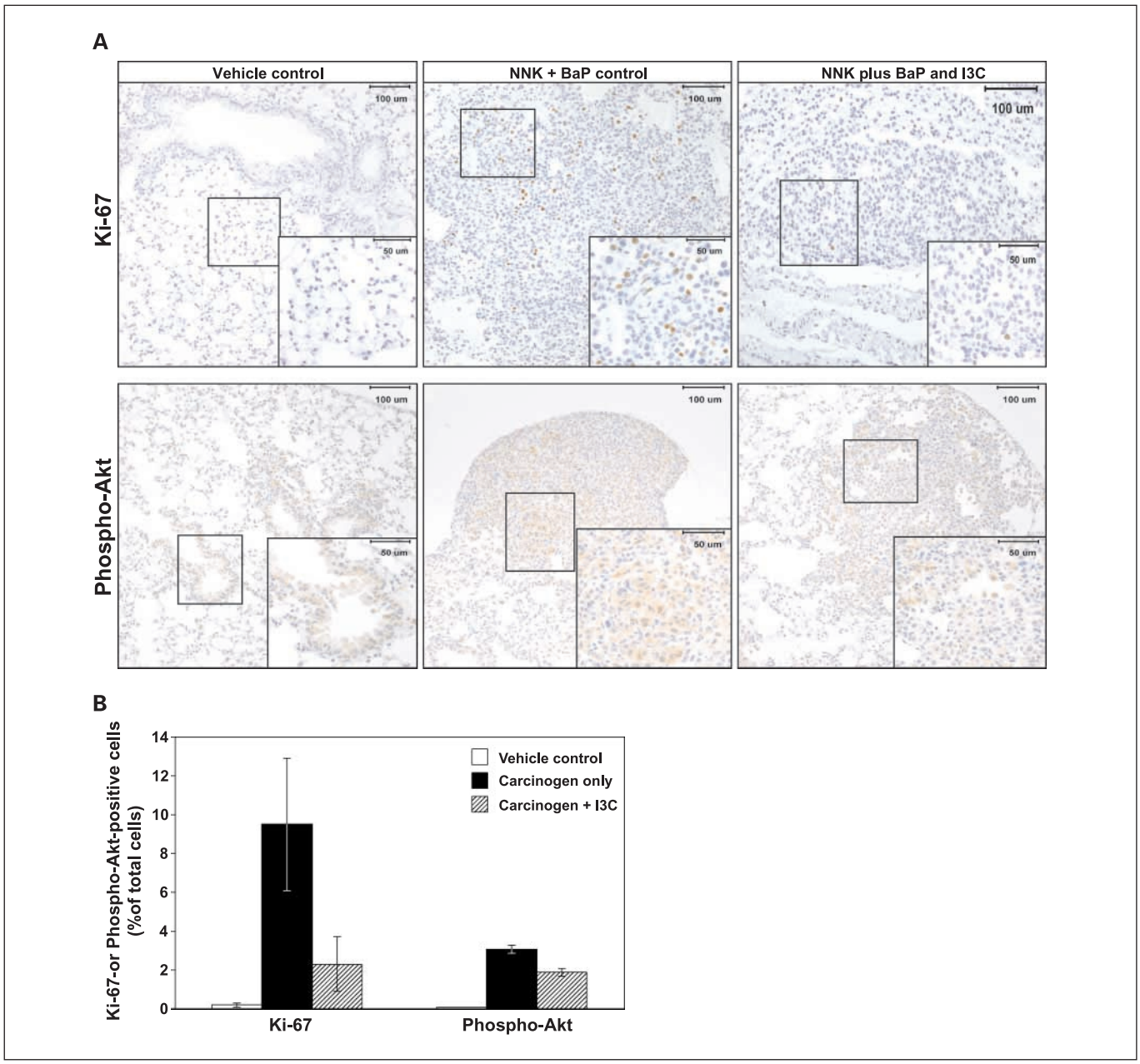

Fig. 4. Effect of I3C on cell proliferation and apoptosis. *A,* photomicrographs (×20) of Ki-67– and phospho-Akt–stained lung tissues from mice treated with vehicle control, NNK plus BaP, or the carcinogens and I3C. Lung tissues obtained from experiment 1 (groups 1, 7, and 9) were cut into 4-μm sections and stained with Ki-67 or phospho-Akt antibody and counterstained with hematoxylin. Images were captured with a camera attached to a Nikon Eclipse E800 microscope. *B,* quantitative assessment of Ki-67– and phospho-Akt–positive cells, representing the percentage of cells that stained positive for Ki-67 or phospho-Akt. The Ki-67 and phospho-Akt labeling index was calculated as described in Materials and Methods. *Insets*, higher magnification of selected areas. *Columns*, mean; *bars*, SD; *, $P < 0.05$.

caused a dose-dependent reduction in the amount of perirenal white adipose tissue. Lower body weight gain and perirenal adipose tissue were not due to reduced food intake because mice given I3C-supplemented diet consumed ~2% to 13% more food than mice maintained on AIN-93 conventional diet. A similar trend in body weight gain was observed in our earlier study in mice (21) as well as in F344 rats. In the latter study, rats given 0.5% I3C in the diet consumed ~13% more diet but mean body weight was ~7% lower compared with group of rats maintained on a control diet (25). The reason for the decrease in body weight gain and depletion of perirenal fat in I3C-treated mice is not known. However, there are two possibilities: increased rate of fat oxidation or decreased fat synthesis. A recent report (26) revealed reduced body weight gain (22%) and adipose tissue (2-fold) in spite of increased food consumption (41%) in mice maintained on soy-supplemented diet, presumably due to preferential use of lipids as energy source and increased locomotor activity. This is typical of phytoestrogens. On the other hand, Maiyoh et al. (27) showed that I3C significantly reduces cellular lipid synthesis, including tryglycerides, and cholesterol esters and the expression of key

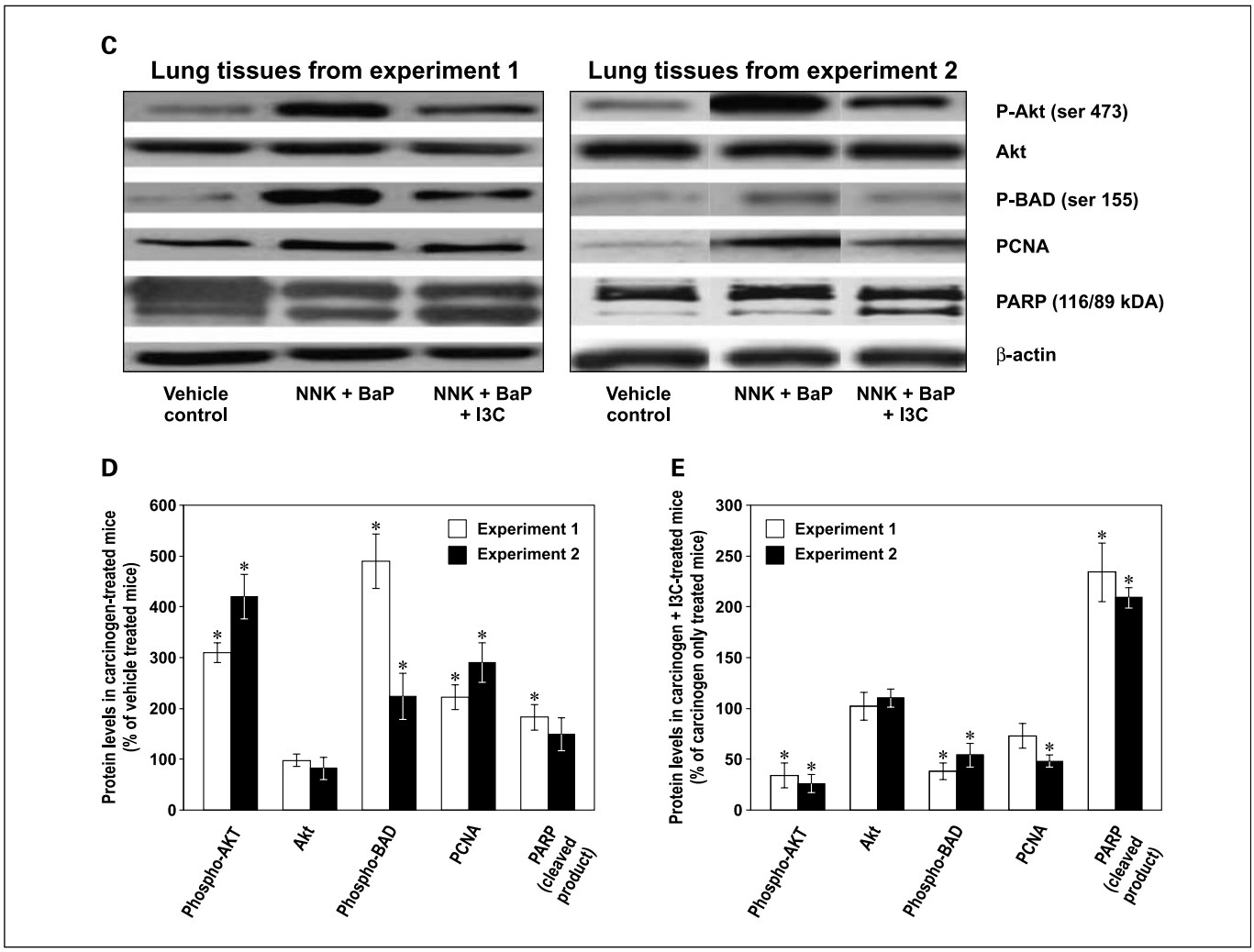

Fig. 4 *Continued. C*, Western immunoblots of lung tissues. Whole lung tissues obtained from experiment 2 or normal lung tissues (group 9) and microdissected tumors (groups 1 and 7) from experiment 1 were prepared as described in Materials and Methods, and equal amounts of protein were loaded onto a 4% to 12% SDS-PAGE followed by immunoblot analysis and chemiluminescence detection. Equal loading of protein was confirmed by stripping the immunoblot and reprobing it for β-actin. *, $P < 0.05$. *D*, mean levels of phospho-Akt, Akt, phospho-BAD, PCNA, and cleaved PARP in lung tumor tissues relative to those in normal lung tissues. *E*, mean levels of phospho-Akt, Akt, phospho-BAD, PCNA, and cleaved PARP in lung tumor tissues from carcinogen and I3C-treated mice relative to those in tumors from mice treated with the carcinogens alone. *, $P < 0.05$.

lipogenic genes, including diacylglycerol acyltransferase, acyl CoA:cholesterol acyltransferase, fatty acid synthase, and sterol regulatory element binding protein, the upstream regulator of fatty acid synthase. We have earlier reported that the NNK plus BaP–induced increase in the expression of fatty acid synthase was reversed by I3C (28). It is not known whether lower body weights in the present study contributed to the chemopreventive activity of I3C. Although calorie restriction is the most potent cancer prevention regimen (29), effects of calorie restriction and reduced body weight gain on lung tumor development have not been extensively studied. In one study, restriction of food intake by 40% and 60% reduced body weight by ~23% and 34%, respectively, but lung tumor multiplicity was reduced only by 25% in both groups (30).

To our knowledge, only four previous reports (21, 31–33) are available on the lung tumor inhibitory effects of I3C in the A/J mouse model. When I3C was given at a dose of 10 or 50 μmol/g diet before a single dose of NNK (31), a moderate 40% reduction in lung tumor multiplicity was observed. Similar results were found upon administration of I3C (13 μmol/g diet) before, during, and after a single dose of NNK (32) or dibenzo(*a,l*)pyrene (33). We have recently shown that a relatively higher dose of I3C (112 μmol/g diet) given in the diet beginning at 1 day after the 4th of eight treatments with a mixture of NNK and BaP reduced lung tumor multiplicity by 86% (21). In the present study, we not only reproduced the above results but also showed that the lung tumor inhibitory activities of I3C are dose dependent and the compound is effective when given during the postcarcinogen treatment phase. Administration of I3C beginning 50% through the carcinogen treatment phase or during the postcarcinogen treatment phase was intended to model, to some extent, smokers transitioning to quitting or former smokers, respectively.

The lowest effective dose of I3C (10 μmol I3C/g diet) corresponds, when compared on the basis of body surface area, to the amount of I3C (800 mg/person, orally) given in phase I

clinical trials (19). This dose of I3C modulated levels of xenobiotic- and steroid-metabolizing enzymes and 2-hydroxyestrone in a manner consistent with chemoprevention without causing toxic effects. It is interesting to note that a dose of I3C that significantly inhibited lung tumor multiplicity in mice without causing toxic effects was well tolerated by humans and modulated levels of chemopreventive agent efficacy biomarkers. This indicates the great potential of I3C for the chemoprevention of lung tumorigenesis in humans.

I3C inhibits tumorigenesis via different mechanisms (9). In studies with cell lines *in vitro*, I3C caused inhibition of cell proliferation through modulation of various proteins involved in cell cycle regulation, induction of proapoptotic proteins, inhibition of antiapoptotic proteins, and inhibition of signaling pathways involved in cell survival such as phosphatidylinositol 3-kinase/Akt and NF-κB (9). In animal models, the main established mechanism by which I3C inhibits tumorigenesis is induction of cytochrome P450 enzymes. I3C inhibited NNK-induced lung tumorigenesis in A/J mice through induction of P450 enzymes, resulting in increased hepatic clearance of the carcinogen through α-hydroxylation and N-oxidation (31). As a result of this, the pulmonary concentration of NNK and its metabolite, NNAL, decreased, and pulmonary DNA methylation, a lesion that leads to lung tumors, was reduced. Recent studies using a mouse model with liver-specific deletion of NADPH–cytochrome P450 reductase, the electron donor for the P450 system, further confirmed the role of P450 enzymes in NNK metabolism (34). Deletion of hepatic cytochrome P450 reductase resulted in decreased P450-mediated hepatic clearance of NNK and a higher multiplicity of NNK-induced tumors in the lung. Similar results were observed in hepatic cytochrome P450 reductase null mice treated with BaP, in which BaP-DNA adduct levels were higher in the liver (up to 13-fold) and elevated in several extrahepatic tissues (by 1.7- to 2.6-fold) of mice with the deleted gene relative to mice with the wild-type gene (35). I3C is known to induce P450s involved in the detoxification of BaP (36, 37).

In the present study, I3C significantly inhibited lung tumor multiplicity when given during the postcarcinogen treatment phase. These inhibitory activities of I3C could be, at least in part, due to inhibition of cell proliferation and induction of apoptosis. NNK plus BaP–induced increases in the frequency of Ki-67–positive cells and PCNA expression, the most common markers of cell proliferation, were reduced by I3C. Also, I3C reduced NNK plus BaP–induced activation of Akt, a cytosolic signal transduction protein that plays an important role in cell survival pathways through inhibition of apoptosis, and its downstream target phospho-BAD. Activated Akt promotes cell survival by phosphorylating and thereby inactivating target proteins such as BAD, which results in dissociation of the protein from the Bcl-2/Bcl-X complex and loss of its proapoptotic function (38). In line with inhibition of Akt and BAD activation, I3C increased cleavage of PARP, a marker of apoptosis. Earlier, I3C was shown to inhibit cell proliferation and induce apoptosis in HPV16-transgenic mice, which develop cervical cancer after chronic estradiol exposure (39, 40), and xenograft models for prostate cancer (41).

In conclusion, we showed that I3C given in the diet beginning at 50% in the carcinogen treatment phase inhibited lung tumorigenesis in A/J mice in a dose-dependent manner. Also, upon administration during the postcarcinogen treatment phase, I3C caused a significant reduction in lung tumor multiplicity and modulated the expression of proteins involved in cell proliferation and apoptosis. These results indicate the potential of I3C for lung cancer chemoprevention in current and former smokers.

Disclosure of Potential Conflicts of Interest

No potential conflicts of interest were disclosed.

Acknowledgments

We thank Mi-ky Lowe for her help in the preparation of the diets and Bruce Lindgren for statistical analyses of the data.

References

1. Parkin DM, Bray F, Ferlay J, Pisani P, et al. Global cancer statistics, 2002. CA Cancer J Clin 2005;55: 74–108.
2. Jemal A, Siegel R, Ward E, et al. Cancer statistics, 2008. CA Cancer J Clin 2008;58:71–96.
3. Hoffmann D, Hoffmann I, El Bayoumy K. The less harmful cigarette: a controversial issue. A tribute to Ernst L. Wynder. Chem Res Toxicol 2001;14:767–90.
4. IARC. Tobacco smoke and involuntary smoking. In: IARC monographs on the evaluation of carcinogenic risks to humans. Lyon: IARC Press; 2004. vol. 83. p. 53-119.
5. Hecht SS. Tobacco smoke carcinogens and lung cancer. J Natl Cancer Inst 1999;91:1194–210.
6. Hecht SS. Biochemistry, biology, and carcinogenicity of tobacco-specific *N*-nitrosamines. Chem Res Toxicol 1998;11:560–603.
7. Malkinson AK. Primary lung tumors in mice as an aid for understanding, preventing, and treating human adenocarcinoma of the lung. Lung Cancer 2001;32:265–79.
8. Bonner AE, Lemon WJ, Devereux TR, Lubet RA, You M. Molecular profiling of mouse lung tumors: association with tumor progression, lung development and human lung adenocarcinoma. Oncogene 2004;23:1166–76.
9. IARC. IARC handbooks of cancer prevention. Cruciferous vegetables, isothiocyanates and indoles. Vol. 9. Lyon: IARC Printing Press; 2004. p. 171-76.
10. Vang O, Dragsted L. Naturally occurring antimutagens. III. Indoles. Copenhagen; Nordic Council of Ministers; 1996.
11. Conaway CC, Getahun SM, Liebes LL, et al. Disposition of glucosinolates and sulforaphane in humans after ingestion of steamed and fresh broccoli. Nutr Cancer 2000;38:168–78.
12. Anderton MJ, Manson MM, Vershoyle RD, et al. Pharmacokinetics and tissue disposition of indole-3-carbinol and its acid condensation products after oral administration to mice. Clin Cancer Res 2204; 10:5233–41.
13. Bjeldanes LF, Kim JY, Grose KR, Bartholomew JC, Bradfield CA. Aromatic hydrocarbon receptor agonist generated from indole-3-carbinol *in vitro* and *in vivo*: comparisons with 2,3,7,8-tetrachlorodibenzo-*p*-dioxin. Proc Natl Acad Sci U S A 1991;88: 9543–7.
14. Hecht SS, Carmella SG, Kenny PMJ, Low SH, Arakawa K, Yu MC. Effects of cruciferous vegetable consumption on urinary metabolites of the tobacco-specificlung carcinogen 4-(methylnitrosamino)-1-(3-pyridyl)-1-butanone in Singapore Chinese. Cancer Epidemiol Biomarkers Prev 2004;13: 997–1004.
15. Broadbent TA, Broadbent HS. The chemistry and pharmacology of indole-3-carbinol (indole-3-methanol) and 3-(methoxymethyl)indole. Curr Med Chem 1988;5:337–52.
16. Sones K, Heaney RK, Fenwick GR. An estimate of the mean daily intake of glucosinolates from cruciferous vegetables in the UK. J Sci Food Agric 1984;35:712–20.
17. Rosen CA, Woodson GE, Thompson JW, Hengesteg AP, Bradlow HL. Preliminary results of the use of indole-3-carbinol for recurrent respiratory papillomatosis. Otolaryngol Head Neck Surg 1998; 118:810–15.
18. Bell MC, Crowley-Nowick P, Bradlow HL, et al. Placebo-controlled trial of indole-3-carbinol in the treatment of CN. Gynecol Oncol 2000;78:123–9.
19. Reed GA, Peterson KS, Smith HJ, et al. A phase I study of indole-3-carbinol in women: tolerability and effects. Cancer Epidemiol Biomark Prev 2005;14:1953–60.
20. Dashwood RH. Indole-3-carbinol:anticarcinogen or tumor promoter in Brassica vegetables? Chem Biol Interact 1998;110:1–5.

21. Kassie F, Anderson LB, Scherber R, Yu N, Lahti D, Upadhyaya P, Hecht SS. Indole-3-carbinol inhibits 4-(methylnitrosamino)-1-(3-pyridyl)-1-butanone plus benzo(*a*)pyrene-induced lung tumorigenesis in A/J mice and modulates carcinogen-induced alterations in protein levels. Cancer Res 2007;67:6502–11.

22. Hecht SS, Lin D, Castonguay A. Effects of α-deuterium substitution on the mutagenicity of 4-(methylnitrosamino)-1-(3-pyridyl)-1-butanone (NNK). Carcinogenesis 1983;4:305–10.

23. Reeves PG, Nielsen FH, Fahey GC. AIN-93 purified diets for laboratory rodents: final report of the American Institute of Nutrition ad hoc writing committee on the reformulation of the AIN-76A rodent diet. J Nutr 1993;123:1939–51.

24. Bogen KT, Witschi H. Lung tumors in A/J mice exposed to environmental tobacco smoke: estimated potency and implied human risk. Carcinogenesis 2002;23:511–19.

25. Jang JJ, Cho KJ, Bae JH. Modifying responses of allyl sulfide, indole-3-carbinol and germanium in a rat multi-organ carcinogenesis model. Carcinogenesis 1991;12:691–95.

26. Cederroth CR, Vinciguerra M, Kühne F, et al. A phytoestrogen-rich diet increases energy expenditure and decreases adiposity in mice. Environ Health Perspect 2007;115:1467–73.

27. Maiyoh GK, Kuh JE, Casachi A, Theeiault AG. Cruciferous indole-3-carbinol inhibits apolipoprotein B secretion in HeG2 cells. J Nutr 2007;137:2185–89.

28. Kassie F, Anderson LB, Higgins L, et al. Chemopreventive agents modulate the protein expression profile of 4-(methylnitrosamino)-1-(3-pyridyl)-1-butanone plus benzo(*a*)pyrene-induced lung tumors in A/J mice. Carcinogenesis 2008;29:610–19.

29. Hursting SD, Lavigne JA, Berrigan D, Perkins SN, Barrett JC. Calorie restriction, aging, and cancer prevention: mechanisms of action and applicability to humans. Annu Rev Med 2003;54:131–52.

30. Stinn W, Teredesai A, Kuhl P, Knoerr-Wittmann C, Kindt R. Mechanisms involved in A/J mouse lung tumorigenesis induced by inhalation of an environmental tobacco smoke surrogate. Inhal Toxicol 2005;17:263–76.

31. Morse MA, LaGreca SD, Amin SG, Chung FL. Effects of indole-3-carbinol on lung tumorigenesis and DNA methylation induced by 4-(methylnitrosamino)-1-(3-pyridyl)-1-butanone (NNK) and on the metabolism and disposition of NNK in A/J mice. Cancer Res 1990;50:2613–17.

32. El Bayoumy K, Upadhyaya P, Desai DH, Amin S, Hoffmann D, Wynder EL. Effects of 1,4-phenylenebis (methylene)selenocyanate, phenethyl isothiocyanate, indole-3-carbinol, and ≻d-limonene individually and in combination on the tumorigenicity of the tobacco-specific nitrosamine 4-(methylnitrosamino)-1-(3-pyridyl)-1-butanone in A/J mouse lung. Anticancer Res 1996;16:2709–12.

33. Yu Z, Mahadevan B, Löhr CV, et al. Indole-3-carbinol in the maternal diet provides chemoprotection for the fetus against transplacental carcinogenesis by the polycyclic aromatic hydrocarbon dibenzo[*a,l*]pyrene. Carcinogenesis 2006;27:2116–23.

34. Weng Y, Fang C, Turesky RJ, Behr M, Kaminsky LS, Ding X. Determination of the role of target tissue metabolism in lung carcinogenesis using conditional cytochrome P450 reductase-null mice. Cancer Res 2007;67:7825–30.

35. Arlt VM, Stiborová M, Henderson CJ, et al. Metabolic activation of benzo[*a*]pyrene *in vitro* by hepatic cytochrome P450 contrasts with detoxification *in vivo*: experiments with hepatic cytochrome P450 reductase null mice. Carcinogenesis 2008;29:656–65.

36. Loub WD, Wattenberg LW, Davis DW. Aryl hydrocarbon hydroxylase induction in rat tissues by naturally occurring indoles of cruciferous plants. J Natl Cancer Inst 1975;54:985–8.

37. Park JY, Bjeldanes LF. Organ-selective induction of cytochrome P-450-dependent activities by indole-3-carbinol-derived products: influence on covalent binding of benzo[*a*]pyrene to hepatic and pulmonary DNA in the rat. Chem Biol Intract 1992;83:235–47.

38. Datta SR, Dudek H, Tao X, et al. Akt phosphorylation of BAD couples survival signals to the cell-intrinsic death machinery. Cell 1997;91:231–41.

39. Chen DZ, Qi M, Auborn KJ, Carter TH. Indole-3-carbinol and diindolylmethane induce apoptosis of human cervical cancer cells and in murine HPV16-transgenic preneoplastic cervical epithelium. J Nutr 2001;131:3294–302.

40. Jin L, Qi M, Chen DZ, Anderson A, Yang GY, Arbeit JM, Auborn KJ. Indole-3-carbinol prevents cervical cancer in human papilloma virus type 16 (HPV16) transgenic mice. Cancer Res 1999;59:3991–97.

41. Souli E, Machluf M, Morgenstem A, Sabo E, Yannai S. Indole-3-carbinol (I3C) exhibits inhibitory and preventive effects on prostate tumors in mice. Food Chem Toxicol 2008;46:863–70.